Am J Cancer Res 2025;15(6):2564-2578
www.ajcr.us /ISSN:2156-6976/ajcr0155674

Original Article

Transcriptomic profiling of PBMCs from mammary tumor dogs reveals two distinct immune states

Kang-Hoon Lee[1*], Dabin Lee[1,2*], Jeong-Woon Lee[1,2], Hyeon-Ji Hwang[1,2], Je-Yoel Cho[1,2]

[1]Department of Biochemistry, BK21 Plus and The Research Institute for Veterinary Science, College of Veterinary Medicine, Seoul National University, Seoul 08826, Republic of Korea; [2]Comparative Medicine Disease Research Center, Seoul National University, Seoul 08826, Republic of Korea. [*]Equal contributors.

Received January 28, 2024; Accepted April 28, 2025; Epub June 15, 2025; Published June 30, 2025

Abstract: This study analyzed cancer-specific systemic immune responses in peripheral blood mononuclear cells (PBMCs) from dogs with benign tumors, malignant tumors, and normal conditions. By examining gene expression patterns - particularly immune checkpoint and TNFRSF genes - the study aimed to assess the immune state of cancer PBMCs. Surprisingly, half of the tumor PBMCs exhibited downregulation of both immunosuppressive genes (Pdcd1, Ctla4, Tigit) and immune activation molecules (CD27, CD357), suggesting immune inactivity rather than suppression. Additionally, cytokine expression varied significantly, with upregulation of IL-18 and IL-7, despite their controversial roles in tumor progression. Analysis of T-cell exhaustion markers did not reflect established exhaustion signatures, implying a naive-like immune state. Instead, a distinct immune signature emerged, characterized by the broad downregulation of TNFRSF genes (TNFRSF18, TNFRSF14, TNFRSF6, and CD27). We designated this group as PI (PBMC-impaired). Deconvolution of bulk RNA-seq data further revealed a significant reduction in CD4+ T cells and a lower CD4+/CD8+ ratio in the PI group. Gene Ontology (GO) and pathway analyses linked CD4+ cell differentially expressed genes (DEGs) to regulatory T-cell differentiation, inflammatory responses, and key immune pathways (IL-2/STAT5, NF-kappa B). Notably, CD7, CXCL6, FASN, FLT3LG, LTB, and TNFRSF18 were significantly downregulated, marking a potential transcriptomic signature of systemic immune impairment. These findings suggest that immune dysfunction in the PI group is not solely attributable to conventional immune suppression but rather to a diminished immune activation state driven by reduced TNFRSF gene expression.

Keywords: Peripheral blood mononuclear cells, PBMC, canine mammary tumor, transcriptome, TNFRSF, TNF receptor superfamily, cancer immunosuppression, single cell RNA-seq

Introduction

Breast cancer (BC) is one of the most common cancers worldwide and remains a leading cause of cancer-related mortality [1]. Despite advances in treatment, early diagnosis, prognosis, and treatment monitoring continue to be critical for improving patient outcomes. BC is a heterogeneous disease with multiple subtypes, and its gene expression profiles are closely linked to prognosis, disease progression, metastasis, and treatment resistance. Clinically, BC is classified based on the expression of estrogen receptor (ER), progesterone receptor (PR), and human epidermal growth factor receptor 2 (HER2), which serve as key factors for both diagnosis and treatment decisions [2].

Cancer biomarkers, which are molecules present in blood, urine, or tissue, play a crucial role in cancer management, including diagnosis, prognosis, treatment response monitoring, and recurrence detection [3]. The American Society of Clinical Oncology (ASCO) recommends the use of CA 15-3, CA 27.29, and CEA as tumor markers. However, these biomarkers have limited utility in early BC diagnosis and recurrence detection [4]. Recent advances in liquid biopsy techniques primarily focus on detecting cancer-derived molecules such as exosomes, cell-free DNA, and circulating tumor cells in blood samples [5]. Addtionally, peripheral blood mononuclear cells (PBMCs) have gained increasing attention as surrogate markers in various diseases, including inflammatory conditions, coronary artery disease, Alzheimer's disease, and

https://doi.org/10.62347/LOJB9067

type 2 diabetes [6]. Multi-omics analyses have revealed that PBMC gene expression and epigenetic modifications change significantly in the presence of malignancies, including hepatocellular carcinoma, non-small cell lung cancer, renal cell carcinoma, BC, and colon cancer [7].

A major driver of PBMC research in oncology is the rising significance of cancer immunotherapy. Immune checkpoint inhibitors (ICIs), such as anti-CTLA-4 and anti-PD-1/PD-L1 antibodies, have revolutionized cancer treatment [8]. However, while ICIs have shown remarkable efficacy in some patients, many others exhibit resistance, underscoring the need for predictive biomarkers and new therapeutic targets. Most research on ICIs has focused on tumor-infiltrating immune cells within the tumor microenvironment (TME), while relatively few studies have explored systemic immune responses in blood [9]. Since tumor-derived signals can induce significant transcriptional changes in circulating immune cells, PBMC transcriptomic profiling has emerged as a promising approach for identifying biomarkers related to cancer progression and immunotherapy responsiveness.

Several studies have attempted to identify BC-related biomarkers by analyzing blood samples. For example, Dumeaux et al. reported an immune dysfunction signature in PBMCs of BC patients, consisting of 50 genes associated with systemic immune suppression [10, 11]. Raiter et al. found that GRP78 expression in PBMCs predicts the benefit of taxane-based neoadjuvant chemotherapy in BC [12]. Additionally, Foulds et al. identified a three-gene signature capable of predicting TNBC relapse using PBMC immunophenotyping and transcriptomic profiling [13]. Furthermore, a decrease in specific immune cell populations, such as natural killer (NK) cells, has been observed in BC patients compared to healthy controls [14]. Despite these findings, studying human clinical samples presents challenges due to sample collection constraints and patient heterogeneity. Animal models are essential for overcoming these limitations; however, conventional BC mouse models have drawbacks. Spontaneous mammary tumors rarely occur in mice, and existing mouse models rely on virus-induced tumors or patient-derived xenografts, which do not fully recapitulate immune-tumor interactions. While humanized mouse models incorporating patient-derived immune and cancer cells are being explored, they remain technically challenging and costly [15]. In contrast, canine mammary tumors (CMTs) closely resemble human BC in terms of spontaneous occurrence, prevalence, underlying mechanisms, and diagnostic markers [16]. Recent advancements in canine omics research have enhanced the utility of dogs as translational models for human diseases, including cancer [17, 18]. Notably, Abadie et al. reported that dogs and CMTs are a strong spontaneous model of human triple-negative breast cancer (TNBC) by showing that more than 76% of CMT are classified as triple-negative through their large cohort study [19]. However, limited studies have investigated immune responses in dogs with mammary tumors, particularly at the systemic level [20].

In this study, we aimed to characterize immune responses to mammary tumors by analyzing PBMC transcriptomic profiles in dogs with mammary tumors as a model for human BC. We performed bulk RNA sequencing (RNA-seq) on PBMCs from dogs with normal, benign, and malignant mammary tumors and identified gene expression signatures correlated with clinical classifications. Using unsupervised clustering of the PBMC transcriptome, we characterized immune states and further refined our findings by deconvoluting bulk RNA-seq data through integration with single-cell RNA-seq (scRNA-seq). To validate our results functionally, we conducted co-culture experiments with a cancer cell lines and PBMCs.

Results

A transcriptional signature in PBMCs differentiates normal from tumor groups but not benign from malignant tumors in Canine Mammary Tumor (CMT) cases

To investigate immune-related transcriptional changes associated with CMT, we performed bulk RNA-seq on PBMCs from 62 dogs, including normal, benign, and malignant CMT cases (**Figure 1A** and Supplementary Figure 1). Our goal was to determine whether systemic immune responses could distinguish tumor-bearing dogs from healthy controls and further differentiate between benign and malignant tumors. Hierarchical clustering of gene expres-

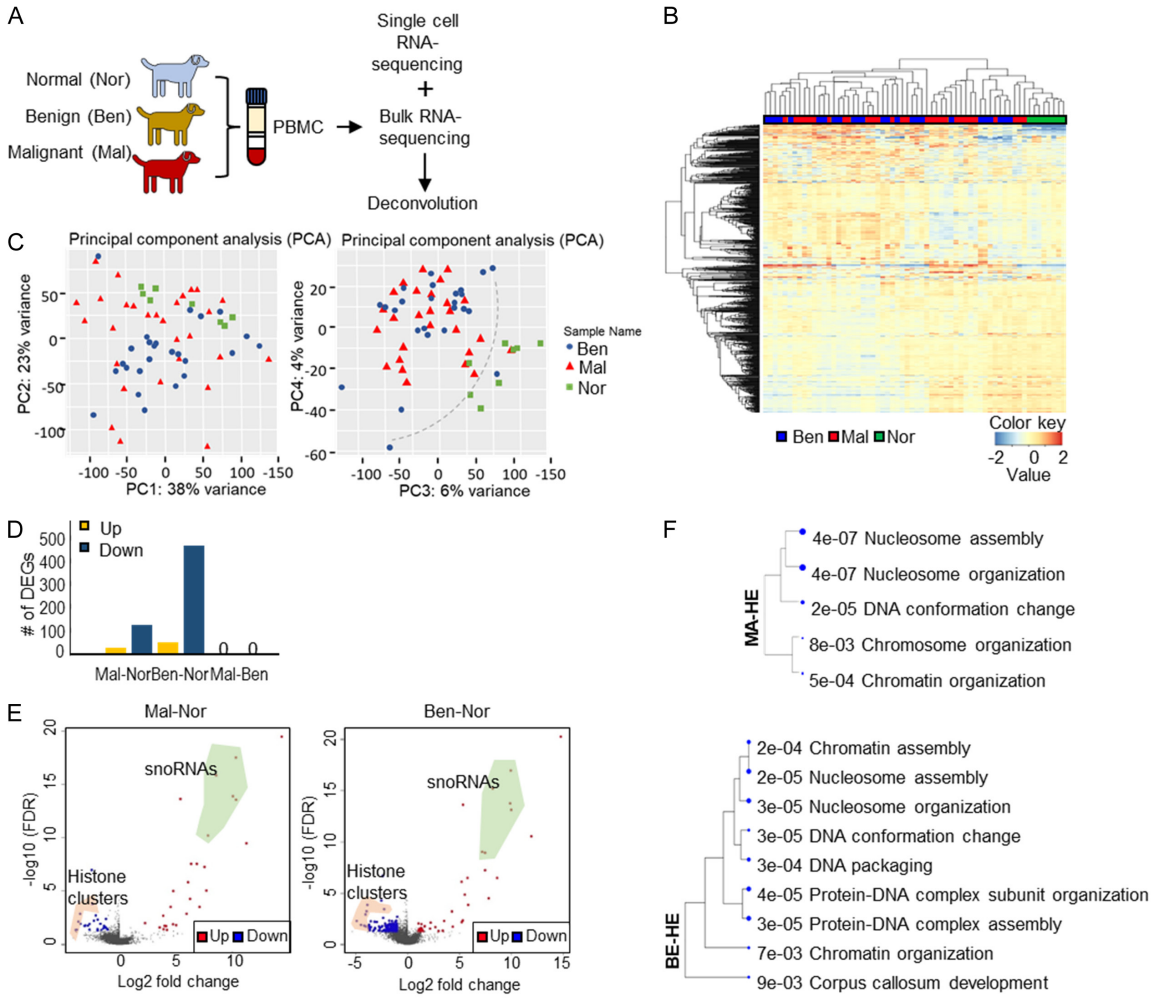

Figure 1. Differentially expressed genes in PBMCs distinguish normal and tumor groups but not benign and malignant in tumor group. A. A schematic diagram of project design. PBMCs were isolated from three groups of dogs, normal, benign, and malignant CMT patients. Gene expression profile was initially analyzed by bulk RNA-seq and deconvoluted by single cell RNA-seq (scRNA-seq) in the representative samples. B. Heatmap clustering separates tumors (malignant and benign) from normal control group. Mal: malignant tumor, Ben: benign, Nor: normal control. C. Principal component analysis (PCA) PC1 and PC2 which represent the most variance (left) and PC3 and PC4 which can separate tumors and normal controls (right). D. Numbers of differentially expressed genes (DEGs) in pairwised comparison, Mal-Nor, Ben-Nor, and Mal-Ben. Yellow bar indicates up-regulated DEGs and navy bar indicates down-regulated DEGs. E. Volcano plots showing each comparison, Mal-Nor (left) and Ben-Nor (right). The x-axis shows fold change (log2 ratio scale) and the y-axis the negative log10 of *p*-values. Green shade indicates snoRNAs and red shade indicates histone cluster genes. Red and blue dots indicate significantly up- and down-regulated genes, respectively. F. The putative functions of highly variable genes in each comparison. Bold indicates terms found in both comparisons, Ben-Nor and Mal-Nor.

sion profiles revealed that PBMC transcriptomes benign and malignant tumors were mixed, whereas normal controls were well-separated (**Figure 1B**). Principal component analysis (PCA) showed that PC1 (38%) and PC2 (23%) failed to separate all three groups, but PC3 (6%) and PC4 (4%) were able to distinguish normal from tumor-bearing dogs (**Figure 1C**). Differential gene expression analysis (FDR = 0.01, |Log2FC| > 1) revealed that the number of differentially expressed genes (DEGs) in the normal vs. benign comparison was approximately 3.6 times greater than in the normal vs. malignant comparison. Notably, the number of downregulated genes was 4 to 9 times higher than the number of upregulated genes. However, no significant DEGs were identified between benign and malignant PBMC transcriptomes, suggesting that systemic immune responses to tumors are similar regardless of

malignancy status (**Figure 1D**). Volcano plot analysis highlighted significant gene expression changes, with remarkable downregulation of histone-related genes and upregulation of small nucleolar RNAs (snoRNAs) in tumor-bearing dogs (**Figure 1E**). Gene ontology (GO) enrichment analysis revealed that downregulated genes were primarily associated with nucleosome assembly and chromatin organization, whereas upregulated genes lacked significant functional categorization except for several snoRNAs (**Figure 1F**).

These findings indicate that while PBMC transcriptomes clearly differentiate tumor-bearing dogs from healthy controls, they do not provide a reliable molecular signature for distinguishing benign from malignant tumors.

Reclassification of immune states in CMT patients using PBMC transcriptome analysis

Given the inability to separate benign from malignant tumors using PBMC transcriptomes (**Figure 1B**), we sought an alternative classification approach based on immune gene expression profiles. Hierarchical clustering of CMT dogs identified two distinct immune subgroups: PBMC Normal-like (PN) and PBMC Impaired (PI). The PN group exhibited transcriptome patterns similar to those of healthy dogs, whereas the PI group displayed a markedly altered immune signature (**Figure 2A**). PCA revealed that PC1 (38%) and PC2 (23%) effectively distinguished the PI group from both normal and PN groups, whereas PN remained intermixed with normal group (**Figure 2B**). Pairwise DEG analysis confirmed that PI PBMCs exhibited significant transcriptomic differences from both normal and PN groups, while PN and normal PBMCs remained highly similar (**Figure 2C**). The PI group exhibited widespread transcriptional downregulation, with 1,462 genes downregulated and only 162 upregulated compared to normal PBMCs. Similarly, 1,341 genes were downregulated and 63 were upregulated in the PI vs. PN comparison (**Figure 2D**). Of these, 1,116 genes (~76% and ~83% of the DEGs in PI-Normal and PI-PN comparisons, respectively) were commonly dysregulated, indicating a strong immune suppression signature in the PI group (**Figure 2E**). These genes were associated with chromatin assembly and immune cell function in the downregulated set, while the upregulated genes were linked to cellular energy metabolism, a pattern that was more pronounced than in the initial tumor-type comparisons (**Figure 2F**).

These results suggest that the immune response in CMT dogs is not significantly determined by tumor type (benign or malignant), and the immune system impaired by tumors has a transcriptional signature that exhibits downregulated epigenetic control and upregulated cell energy metabolism status.

Complex immune state with significant reduction of Tumor Necrosis Factor Receptor Superfamily (TNFRSF) genes in the PI group

We analyzed gene expression patterns across our redefined groups to investigate their association with various immune states. Initially, we examined the expression of immune checkpoint genes, which play a crucial role in anticancer immunotherapy. Surprisingly, the expression of representative immune checkpoint genes (Pdcd1, Ctla4, and Tigit) was downregulated in the transcripts of PI groups that were distinct from normal (**Figure 3A**). In addition, major immuno-activating molecules, including CD27 (TNFRSF7) and CD357 (GITR or TNFRSF18), also showed decreased expression in PI groups (**Figure 3B**). These findings suggest that the immune checkpoint gene expression pattern of PI groups reflects immune inactivity rather than active immunosuppression (**Figure 3A**, **3B**).

Next, we examined the expression of representative cytokines in the PN and PI groups. Six cytokines - IL-7, IL-11, IL-16, IL-18, IL-33, and IL-34 - showed significant differences in expression between the groups. Among them, IL-33 and IL-11 had low expression levels, making their functional relevance unclear. Additionally, the roles of the remaining four cytokines in the PI group were ambiguous: while the pro-tumoral cytokines IL-16 and IL-34 were downregulated, IL-18 and IL-7 were upregulated. Although IL-18 and IL-7 are traditionally associated with antitumor effects, recent studies have suggested their potential pro-tumoral roles. Further analysis is needed to determine how their increased expression affects patient PBMCs (**Figure 3C**).

T-cell exhaustion is a well-characterized immune state in cancer therapy, marked by a

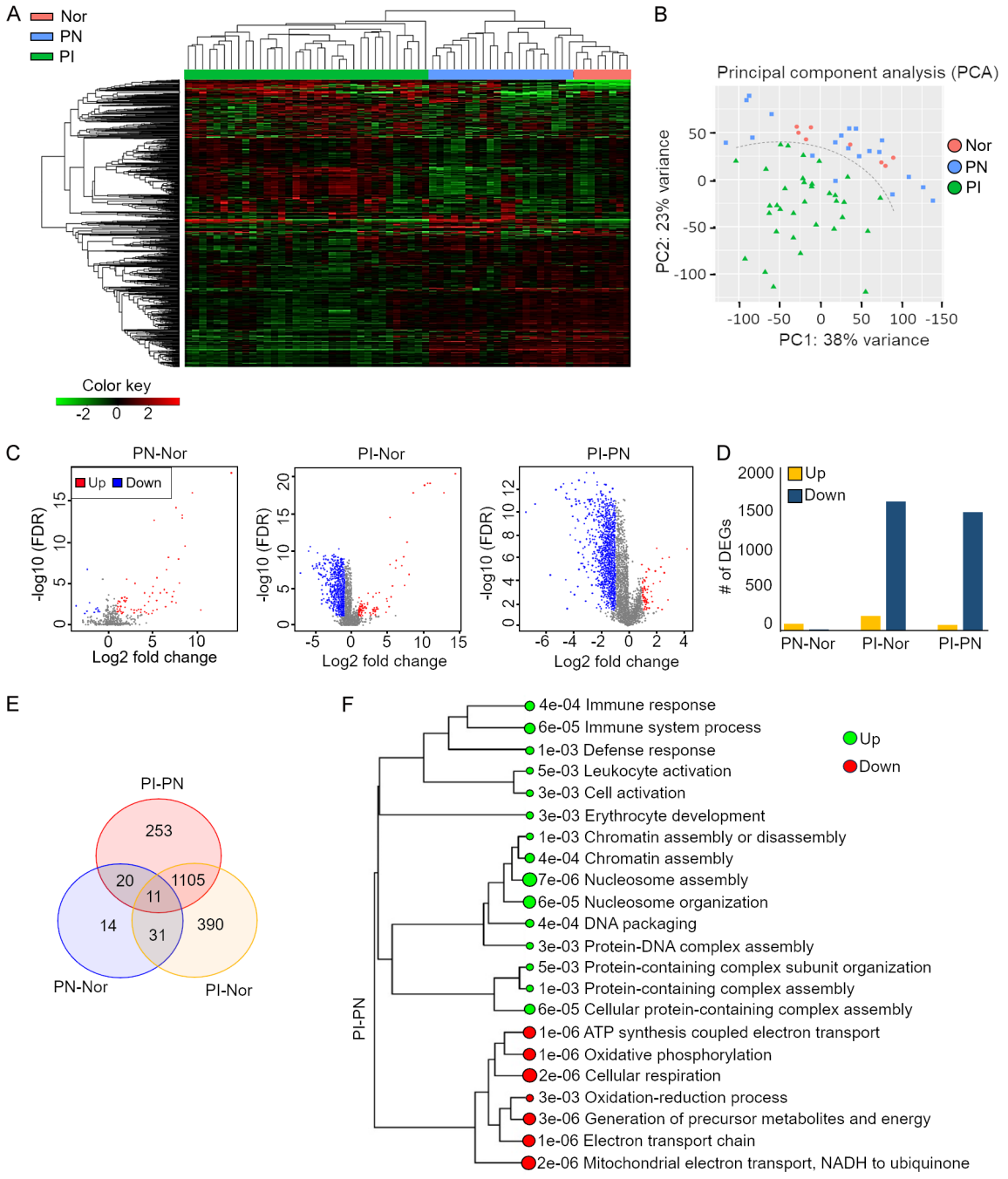

Figure 2. Transcriptome signature classified immune states of PBMC in tumor patient dogs. A. Hierarchical clustering followed by heatmap re-defines three groups based on PBMC transcriptome. Nor: normal control, PN: PBMC Normal-like, PI: PBMC Impaired by tumors. B. PCA separates Nor and PN group from PI group. C. Volcano plots presenting three comparisons, PN-Nor (left), PI-Nor (middle), PI-PN (right), numbers of down-regulated genes (blue dots) were more than up-regulated genes (red dots) in PI group. D. The number of differentially expressed genes (DEGs) found in three comparisons. The yellow bar indicates up-regulated genes, and the navy bar indicates down-regulated genes. E. Venn diagram shows numbers of DEGs among three comparisons. F. The putative functions of DEGs in PI-PN comparison. Green dots indicate terms of down-regulated genes and red dots up-regulated genes. The size of dots indicate significance.

decline in effector T-cell function, persistent expression of inhibitory receptors, and distinct transcriptional profiles [21]. To assess whether the PI group exhibited signs of T-cell exhaus-

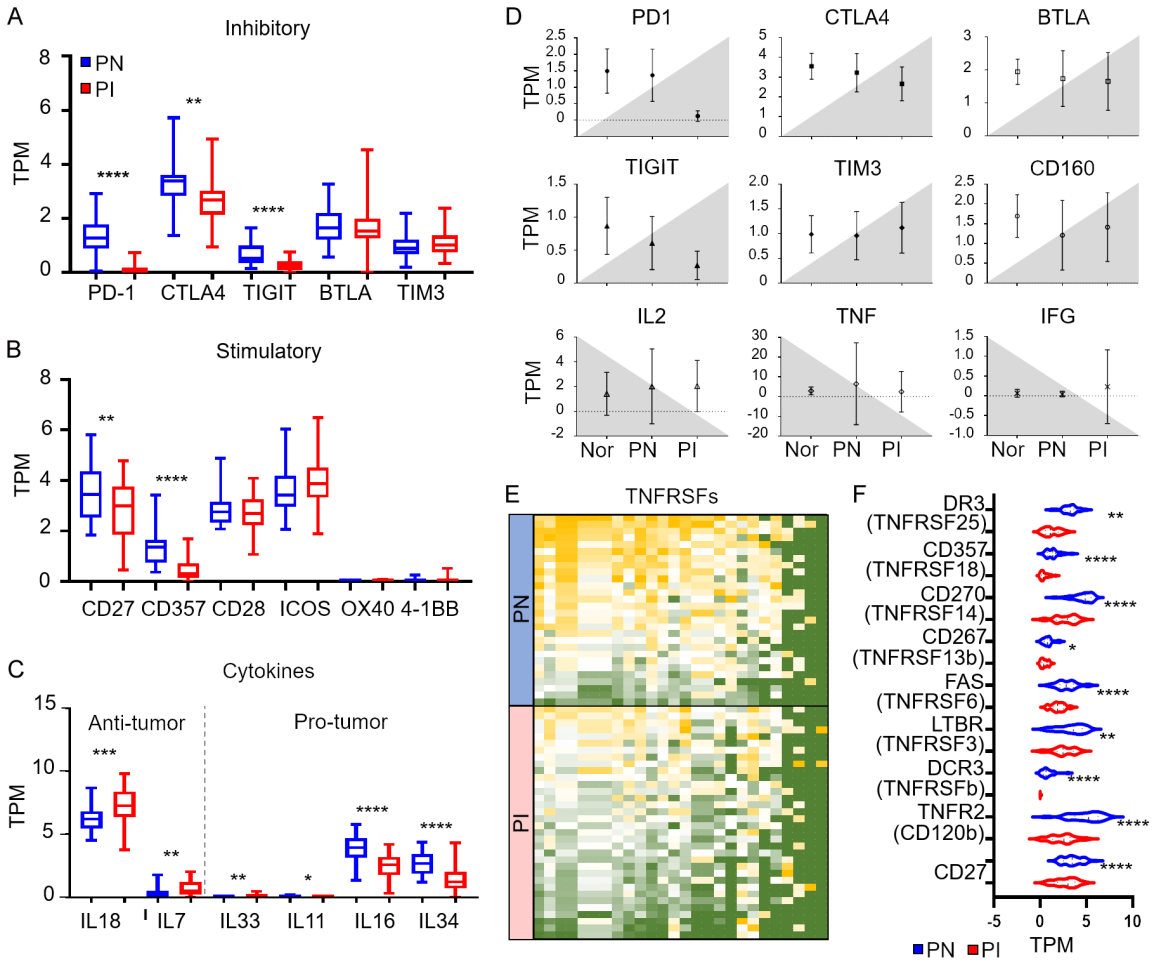

Figure 3. Both immune-suppression and activation signals are down-regulated in PI transcriptome. Gene expression levels in both PI and PN was depicted by box and whisker plots (A) in five inhibitory immune checkpoint molecules (ICMs), (B) six immune activation molecules, and (C) anti- and pro-tumorigenic cytokines. Blue: PN, red: PI. (D) Gene expression levels were compared with known nine T-cell exhaustion signature genes. Gray shade indicates expected gene expression pattern in T-cell exhaustion condition. (E) Twenty-six TNFRSF gene expressions was found in the PN and PI groups of PBMC in dogs. Yellow: high gene expression; green: low gene expression. (F) Violin plots showed significantly different expression of nine TNFRSF genes between PI and PN groups. Asterisks indicate *p*-value < 0.05, **: 0.01, ***: 0.001 and *: 0.0001. Blue: PN, red: PI.

tion, we compared our transcriptome data with established T-cell exhaustion markers (**Figure 3D**). However, the gene expression patterns in the PI group did not align with known exhaustion markers. The consistently low levels of PDCD1, CTLA4, and TIGIT suggested that T cells in PI-group were in a naive-like state rather than experiencing exhaustion.

Instead, we identified a distinct gene signature in the PI group, particularly a significant reduction in TNFRSF (Tumor Necrosis Factor Receptor Superfamily) gene expression (**Figure 3E**). Analysis of 26 TNFRSF genes revealed a broad downregulation in the PI group, with violin plots highlighting notable differences in the expression of nine TNFRSF genes (**Figure 3F**). Among these, TNFRSF18, TNFRSF14, TNFRSF6, TNFRSFb, CD120b, and CD27 were significantly downregulated. These findings indicate that the systemic immune response in the PI group differs substantially from that of tumor-infiltrating lymphocytes (TILs) and cannot be solely attributed to immune cell suppression or T-cell exhaustion via conventional immune checkpoint mechanisms. On the other hand, the distinct TNFRSF gene expression profile suggests a diminished capacity for immune activation in the PI group.

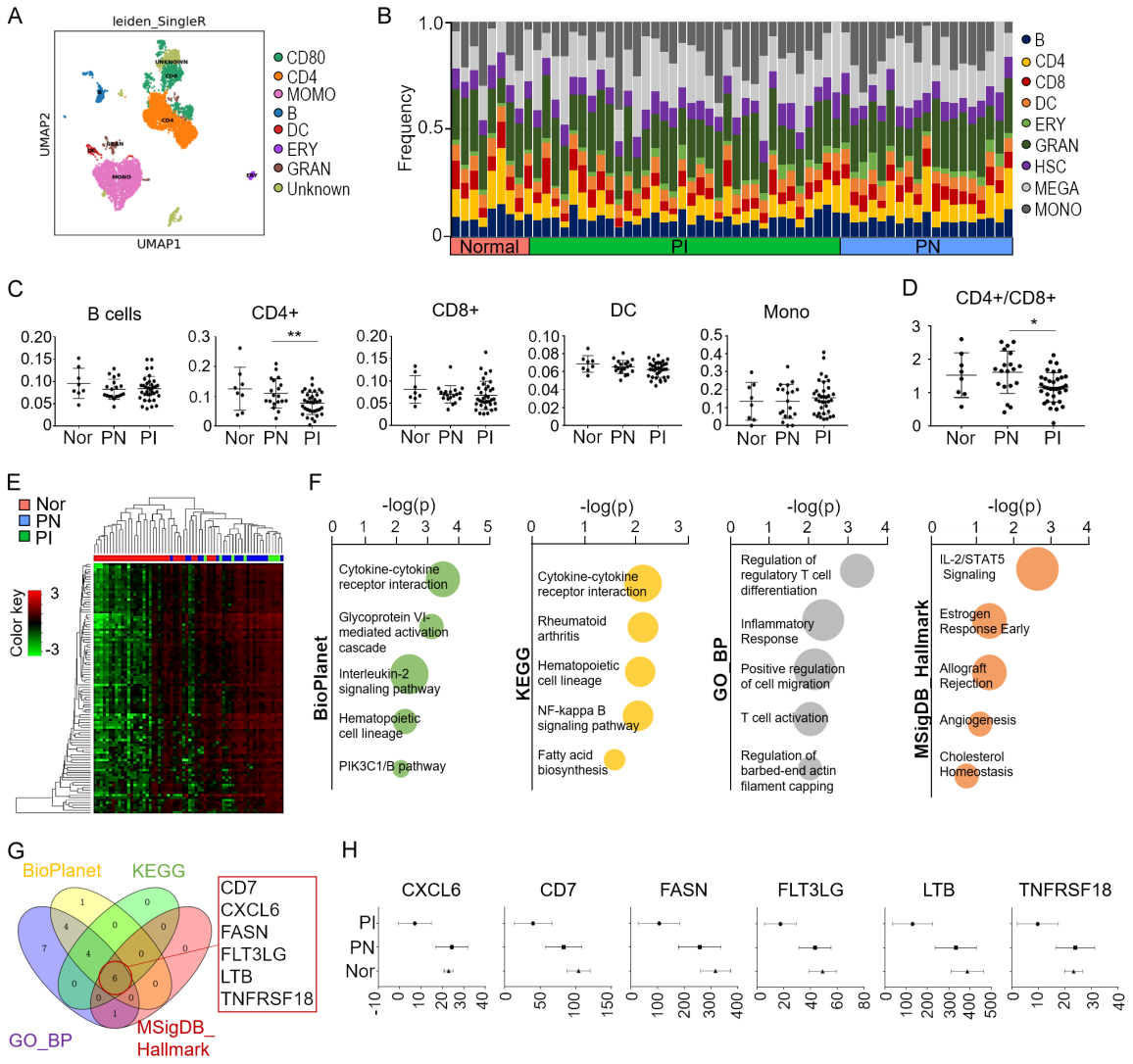

Figure 4. Cell type deconvolution revealed that CD4+ cells are significantly arrested by tumors in PI group and suggested six key molecules which are involved in the process and have crucial roles in the CD4+ cells responding to tumor cells. (A) Single cell RNA-seq (scRNA-seq) of dog PBMCs of normal and CMT resulted in the UMAP plot of dog PBMCs representing tumor and normal conditions with 8 major clusters/cell types. (B) One hundred percent stacked bar chart displayed cell type composition in each PBMC sample. Each color represents cell type. Scatter dot plot together with mean values and standard deviation (SD) showed in (C) five major cell types and (D) the ratios of CD4+ and CD8+ cells in three groups, Nor, PN and PI. (E) Hierarchical clustering and heatmap using DEGs in CD4+ cells tend to separate PI from PN and Nor groups. (F) Top five terms in the pathway and gene enrichment analysis using the DEGs in CD4+ cells. (G) Venn diagram identified six genes (*CD7, CXCL6, FASN, FLT3LG, LTB and TNFRSF18*) enriched in the top five terms from four different libraries, BioPlanet, KEGG, GO_BP, and MSigDB Hallmark. (H) The differential gene expressions of six genes depicted by mean values with SD in three groups.

Deconvolution of bulk RNA-seq data reveals predominant impact on CD4+ T cell populations in PI group

PBMCs represent a heterogeneous population of immune cells. The advent and affordability of single-cell sequencing technology have enabled its widespread use in immunological studies. In this study, we conducted bulk RNA-seq of PBMCs for further applications including clinical uses, followed by deconvolution at the single-cell level to determine the contributions of different PBMC cell types to transcriptional profiles across normal, benign, and malignant tumors, as well as between the PI and PN groups.

Since single-cell RNA sequencing (scRNA-seq) data from the PBMCs of CMT dogs were unavailable, we generated scRNA-seq data from PBMCs of normal and CMT dogs as a reference (**Figure 4A**). Using this dataset, we identified eight major immune cell types - T cells, B cells, monocytes, macrophages, dendritic cells, eosinophils, and neutrophils-based on human immune cell expression profiles. Deconvolution was performed using the CIBERSORTx program (**Figure 4B**) [22].

While no significant differences were observed in cell type distribution across the original tumor-type classification (normal, benign, malignant) (Supplementary Figure 2), PBMC transcriptome-based classification (normal, PN, PI) revealed a significant reduction in CD4+ T cells in the PI group compared to the normal and PN groups (**Figure 4C**). Furthermore, the CD4+/CD8+ cell ratio, a key factor in assessing immunosuppressive states, was significantly lower in the PI group (**Figure 4D**) [23]. Although DEGs in CD4+ cells partially distinguished the PI group from the PN and normal groups, other cell types likely also contribute to the bulk PBMC transcriptomic response to tumors (**Figure 4E**).

GO analysis of DEGs in CD4+ cell populations revealed enrichment in pathways related to regulatory T-cell differentiation, inflammatory response, positive regulation of cell migration, T-cell activation, and actin filament capping. BioPlanet and KEGG pathway analyses further identified immune-related pathways such as cytokine-cytokine receptor interaction, interleukin-2 signaling, and NF-kappa B signaling. The MSigDB hallmark database, which catalogs well-defined biological states, highlighted IL-2/STAT5 signaling, early estrogen response, and allograft rejection (**Figure 4F**).

To identify PI signature genes driving these biological functions, we analyzed 23 candidate genes. Six genes - CD7, CXCL6, FASN, FLT3LG, LTB, and TNFRSF18 - were consistently implicated across all four databases (**Figure 4G**). The expression levels of these six genes were significantly lower in the PI group compared to the PN and normal groups (**Figure 4H**). However, it is unclear in tumor-based classification (Supplementary Figure 3).

Overall, the downregulation of these genes in CD4+ T cells may serve as a critical transcriptomic signature representing systemic immune impairment caused by the tumor.

Co-culture of PBMCs with cancer cells mimics systemic immune suppression

To further investigate the immune suppression signature observed in PBMCs from CMT dogs, we established an in vitro co-culture model to assess the functional impact of cancer cells on T-cell activity. CD3+ T cells were isolated from human PBMCs and co-cultured either directly with cancer cells or indirectly with cancer cell-conditioned medium. Our results demonstrated that T-cell suppression was proportional to the cancer/T-cell ratio and the concentration of cancer cell-derived factors, with higher cancer cell numbers and increased conditioned medium leading to greater suppression (**Figure 5A**, **5B**).

To determine whether this suppression was linked to cell cycle arrest, we analyzed cell cycle distribution after 48 hours of co-culture. T cells co-incubated with cancer cells exhibited a significant accumulation in the S-phase, with an approximately 2.2-fold increase compared to T cells co-cultured with normal cells (**Figure 5C**, **5D**). This finding suggests that cancer cells impair T-cell proliferation by inducing cell cycle arrest in the S-phase, potentially leading to reduced immune responsiveness.

Next, we examined the expression of six key immune-related genes in CD4+ T cells co-cultured with cancerous and non-cancerous cells. Compared to the control group, where T cells were co-cultured with non-cancerous cells, four genes - CD7, FLT3, LTB, and TNFRSF18 - were significantly downregulated in the cancer co-culture condition. In contrast, FASN showed no significant change, and CXCL6 was undetectable (**Figure 5E**). Further analysis of genes associated with T-cell activation and suppression revealed that CD27 (T-cell activation) [24] and TIGIT (immune suppression) [25] were significantly downregulated in the cancer co-culture condition, mirroring the transcriptomic pattern observed in PBMCs from the PI subset. Notably, IL-7, an anti-tumoral cytokine that was upregulated in the PBMC analysis, exhibited a

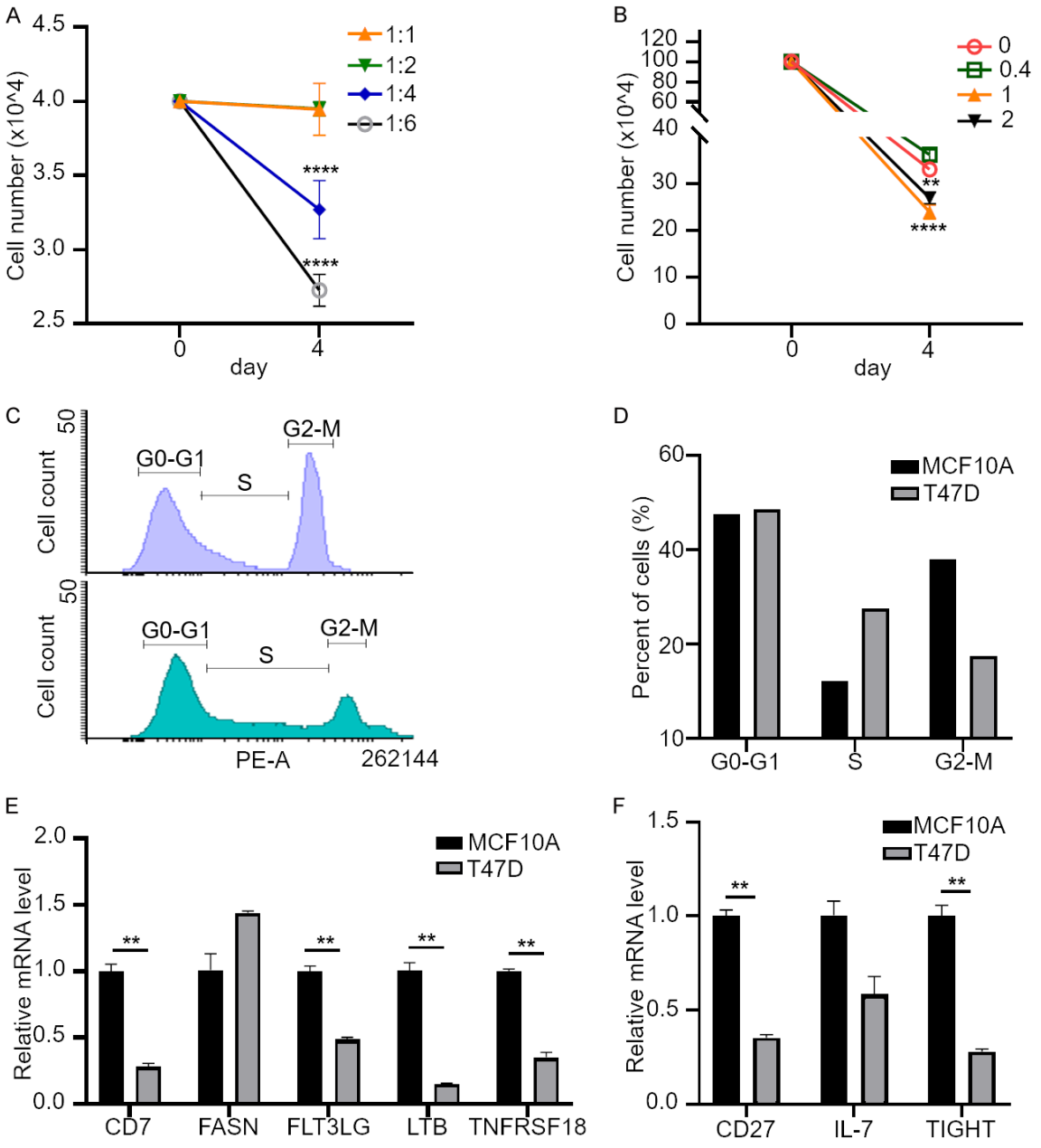

Figure 5. *In vitro* co-culture using PBMCs/T-cells with tumor cells mimics immune cell suppression via S-phase arrest. PBMCs are arrested by the co-culture with tumor cells depending on (A) the numbers of tumor cells and (B) the proportion of tumor conditioned media for 4 days. (C) The cell cycle distribution of T-cells after co-culture with MCF10A normal cells (top) and T47D breast cancer cells (bottom). (D) Tumor cells co-culture induced S-phase arrest in T-cells. Down-regulation of (E) five signature gene expression and (F) three immune stimulators was confirmed *in vitro* co-culture system. Asterisks (**) indicates *p*-value < 0.01.

decreasing trend in the co-culture model, though the change was not statistically significant [26] (**Figure 5F**).

These findings indicate that co-culture of T cells with cancer cells effectively replicates the systemic immune suppression signature observed in PBMCs from CMT patient dogs. The down-regulation of both stimulatory and inhibitory immune-related genes suggests a state of immune paralysis, rather than classical T-cell exhaustion.

Discussion

Over the past few decades, significant advances have been made in the development of anticancer drugs, with a particular focus on immuno-oncology [27]. Third-generation immunotherapies, which aim to block cancer cell signals that enable immune evasion, have gained considerable attention [28]. Since the FDA approved Yervoy in 2011, and Keytruda and Opdivo in 2014 for the treatment of malignant melanoma, numerous cancer drugs targeting PD-1, PD-L1, CTLA-4, and LAG3 have been approved [29]. Despite these advances, the effectiveness of these immunotherapies remains limited, benefiting only about 20% of patients [30]. One major factor influencing the efficacy of ICIs is the TME, which can either support or suppress anti-tumor immune responses [31]. Tumors with an immune-excluded or immune-desert phenotype often exhibit poor responses to ICIs, as seen in TNBC [32]. Due to its highly immunosuppressive TME, TNBC is generally resistant to ICI treatment, highlighting the need for a deeper understanding of the interplay between cancer and the immune system.

Our study focuses on CMT, which share many biological and immunological similarities with TNBC [19]. Notably, we have identified a distinct subset of CMT dogs (PI) (~50%) exhibiting a profound immune suppression signature, characterized by the downregulation of multiple immune-related genes. This finding suggests that, like TNBC, a significant proportion of CMT cases may have an immunosuppressive TME that limits ICI efficacy. Understanding the mechanisms driving this immune suppression could provide valuable insights into overcoming resistance to immunotherapies in both canine and human cancers.

Although our findings suggest immune suppression rather than exhaustion in CMT, previous human studies, such as those by MacFarlane IV et al., have reported a systematic increase in blood PD-1 levels at advanced stages of human renal cancer [33]. Several factors could explain these differences.

First, variations in cancer stage and type must be considered, as these factors significantly impact immune checkpoint gene expression. Many human studies reporting elevated PD-1/CTLA-4 levels have focused on patients with advanced-stage tumors characterized by severe immune depletion and an immunosuppressive TME [34]. In contrast, CMT presents various tumor subtypes and stages, some of which resemble TNBC - a form of breast cancer known for its poor response to PD-1/PD-L1 inhibitors. These variations could significantly influence immune checkpoint expression.

Second, the tissue origin of immune cells plays a crucial role. While PD-1/CTLA-4 upregulation is frequently observed in TILs within the TME, PBMCs may not always reflect the same level of immune activation or inhibition [35]. Thus, systemic immune responses detected in PBMCs may differ from localized immune responses within the tumor.

Third, if a benign tumor persists for a long time, it may induce immune cell changes in the blood that resemble those observed in cancer patients. Specifically, chronic inflammation, an increase in immunosuppressive cells, and T cell exhaustion may occur. However, the extent of these changes is likely to be less pronounced than in malignant tumors, and the degree of immune modulation may vary depending on the type and location of the benign tumor. In canine mammary tumors, diagnosis is often delayed, and the disease progresses for a long time before detection. As a result, even benign tumors in dogs may exhibit immune profiles similar to those of malignant tumors. To investigate this further, experimental approaches analyzing immune cell profiles in the blood of dogs with benign mammary tumors and comparing them to those of malignant cases would be necessary. Studies focusing on specific benign tumor types (e.g., long-standing adenomas or fibromas) could provide valuable insights.

Lastly, species-specific immunomodulatory mechanisms may contribute to the observed differences [36]. There is still a possibility that the immune landscape in dogs and humans may differ in ways that affect PD-1/CTLA-4 regulation and overall immunotherapy responses.

From a more clinical perspective, our findings revealed an increase in C-reactive protein (CRP) and a decrease in total bilirubin (T. bilirubin) levels in the PI group (Supplementary Figure 4). CRP is a well-established marker of systemic

inflammation, often linked to immune activation and tumor progression [37]. Conversely, decreased T. bilirubin levels may indicate reduced antioxidant capacity, which could enhance immunosuppression and susceptibility to oxidative stress in cancer. This paradoxical combination of elevated inflammatory markers alongside potential immune suppression underscores the complexity of immune regulation in cancer [38]. These findings suggest that systemic inflammation does not necessarily equate to effective anti-tumor immunity. Further studies incorporating PBMC transcriptomics and functional immuno assays are needed to clarify these observations in both canine and human BC models.

This study includes additional factors that further increase its complexity and should be considered for a better understanding of the results. From the perspective of tumor heterogeneity, the canine mammary tumor (CMT) samples used in this study encompass various subtypes of CMT (Supplementary Figure 1). These diverse subtypes can significantly influence the tumor microenvironment (TME) through differences in cellular composition and the infiltration of immune cells. Furthermore, interactions between immune cells and tumor cells within the TME, the types of cytokines expressed, and the inflammatory response can also be affected. In addition to these factors, other variables such as hormonal differences due to neutering, breed-specific variations, and age-related factors should also be taken into account. Nevertheless, CMT remains an attractive model for research due to its similarity to triple-negative breast cancer (TNBC) and the ability to simplify cohort selection, thereby reducing heterogeneity compared to human studies.

In the PI group, transcriptomic changes were predominantly related to immune system functions and epigenetic modifications, including alterations in chromatin assembly and protein-DNA complexes. These epigenetic changes play crucial roles in inflammation and immune responses, which are key to cancer initiation and progression. Notably, immune checkpoint molecules such as PDCD1 (PD-1), CTLA-4, TIM-3 (HAVCR2), LAG3, and TIGIT are regulated by epigenetic mechanisms, highlighting their potential as therapeutic targets for cancer immunotherapy [39]. Furthermore, we observed a significant reduction in TNFRSF family members (TNFRSF25, TNFRSF18, TNFRSF14, TNFRSF13B, TNFRSF6, TNFRSF3, TNFRSF1B, and CD27), immune checkpoint molecules (PD-1, CTLA-4, TIGIT), and cytokine-related genes (IL-16, IL-34). These findings suggest a systemic immunosuppressive state that may hinder effective anti-tumor immunity. Given the critical role of TNFRSF members in T cell activation and survival, their downregulation indicates impaired T cell homeostasis [40]. Additionally, the reduction in IL-16 and IL-34, which are essential for immune cell recruitment and antigen-presenting cell (APC) function, suggests a failure in immune communication [41, 42]. Our findings support the notion that CD4+ T cells, often considered 'helper cells', play a more prominent role in immune responses than previously thought. The suppression of CD4+ T cells in the PI group further underscores the complexity of immune regulation in cancer. ScRNA-seq and deconvolution analysis revealed a significant reduction in CD4+ T cells in a subset of CMT patients, with signature genes closely correlated those of Th1-like CD4+ T cells. This finding suggests that a distinct group of CMT dogs may experience depletion of Th1-like CD4+ cells, which play a crucial role in orchestrating anti-tumor immune responses [43] (Supplementary Figure 5). Given the importance of Th1-mediated immunity in enhancing cytotoxic T cell activity and improving responses to ICIs, the loss of this subset may contribute to immune evasion and reduced therapeutic efficacy. Notably, the expression of PI signature genes showed a significant negative correlation with survival in several types of human cancers, including breast cancer (BC), head and neck squamous cell carcinoma (HNSC), and skin cutaneous melanoma (SKCM) (Supplementary Figure 6A). Furthermore, BC patients with high PI signature genes' expression showed better overall survival, highlighting its potential prognostic significance in breast cancer (Supplementary Figure 6B). This observation aligns with findings in TNBC, where an immunosuppressive tumor microenvironment limits ICI effectiveness. Understanding the mechanisms underlying Th1-like CD4+ cell depletion could provide valuable insights into resistance to immunotherapies and inform novel strategies to enhance treatment responses in both canine and human cancers.

Overall, our study suggests that CMT may serve as a valuable model for understanding resistance mechanisms in TNBC and other BC subtypes that show limited responses to PD-1/PD-L1 blockade. The observed immune profiles in PBMCs provide potential insights into systemic immune dysregulation in tumors that do not respond well to ICIs. Given the growing concern over resistance to anti-PD-1 therapy, our findings may provide insights into patient populations less likely to respond to ICIs. The identified PBMC gene expression changes could serve as potential biomarkers for predicting immunotherapy outcomes. Further research is needed to validate these findings and explore novel immunotherapeutic strategies to overcome resistance to ICIs in both CMT and BC.

Materials and methods

Animal specimens and PBMC isolation

All companion dogs were enrolled and processed with the approval of the Institutional Animal Care and Use Committee (IACUC) of Seoul National University (IACUC SNU-170602-1). Blood samples were collected in ethylenediaminetetraacetic acid (EDTA) tubes. PBMC were isolated from approximately 2 to 5 ml of blood with a 2X volume of Ficoll Paque PLUS (GE Healthcare, Chicago, IL, USA) and centrifuged at 400×g, followed by washing with phosphate-buffered saline (PBS). PBMCs were stored at -80°C until RNA isolation. Brief information on companion dogs is provided in Supplementary Figure 1A.

RNA isolation and total- and single cell-RNA (scRNA) sequencing

Total RNA was extracted from PBMCs of CMT and normal dogs using the RNeasy Mini Plus kit (Qiagen, Hilden, Germany). Total RNA sequencing was performed as previously reported by our group [44]. PBMCs were freshly isolated from two Pomeranian dogs, one healthy dog, and one dog with CMT. The cell pellet was incubated with 5 mL RBC lysis buffer at room temperature for 2 min. Cells were washed with an ice-cold resuspension buffer (0.5% bovine serum albumin (BSA) in 1× PBS) for two times at 300×g for 5 min. Cell number and viability were analyzed using a Bio-Rad cell counter (Bio-Rad, Hercules, CA, USA). Approximately 3000-5000 single cells with greater than 70% viability were subjected to library preparation. The 10x barcoding and complementary DNA (cDNA) synthesis was performed using the 10x chromium single cell 3' V3 chemistry according to the manufacturer's instructions. The libraries were sequenced using the Illumina Nova6000 according to the recommended specifications (Ebiogen Inc., Seoul, South Korea).

Transcriptome profiling

Initially, to count the expression and generate a bam file, raw sequence files were trimmed using Trimmomatic (ver. 0.39) and aligned using STAR (ver. 2.7.1a) in the RSEM (ver. 1.3.1). Subsequently, the BAM file was preprocessed by sorting and indexing using the same tool (ver. 1.7) to be subject to bamCoverage (ver. 3.3.2). Normalized expression data were applied to the iDEP (integrated Differential Expression and Pathway analysis) to obtain a heatmap, PCA, and differentially expressed genes (DEG) (http://bioinformatics.sdstate.edu/idep/) [45]. The top five representative terms were presented in various libraries, including BioPlanet, KEGG, GO, and MsigDB Hallmark using EnrichR (a web server for comprehensive gene set enrichment analysis: https://maayanlab.cloud/Enrichr/) [46]. Raw data concerning this study have been submitted under SRA accession number SRR23336423-SRR23336486.

Correlation and survival analysis

The correlation between the expression of six signature genes and the signatures associated with T cell characteristics was analyzed using blood samples from the GTX database through GEPIA2 (http://gepia2.cancer-pku.cn/). Pearson's correlation method was used to calculate the correlation coefficients. Additionally, an overall survival (OS) analysis was conducted across 33 cancer databases to examine the relationship between gene expression and survival. Positive and negative correlations were represented in red and blue, respectively, with unique differences highlighted by red and blue borderlines. Among these, the OS for BC was specifically illustrated using a Kaplan-Meier survival plot.

Immune cell type deconvolution by CIBERSORTx

Normalized gene expression data from bulk RNA-seq were used to infer the estimated proportions of immune cells using the CIBERSORTx algorithm [47]. This used a set of reference gene expression values. Before deconvolution, we generated a signature matrix using the scRNA-seq data of normal and cancerous PBMCs. Leiden clustering was performed to group the cell types, and each cell type was characterized using high-rank gene expression. Canine scRNA-seq data were annotated using the SingleR library (v.1.6.1) and the DMAP database. Finally, based on human immune cell expression profiles, we defined eight major immune cell types, including subsets of T cells, B cells, monocytes, macrophages, dendritic cells, eosinophils, and neutrophils in canine PBMCs.

Cell culture

All cell lines and primary cells were purchased from the Korean Cell Line Bank (Seoul, South Korea) or the American Type Culture Collection (ATCC). The normal breast cancer cell line MCF10A was cultured in mammary epithelial cell growth medium (Lonza, Basel, Switzerland). Roswell Park Memorial Institute 1640 medium (Hyclone, UT, USA) was used to culture SKBR-3 and T47D cells. Primary T cells were maintained RPMI1640 medium, supplemented with 10% fetal bovine serum (FBS) and 1% penicillin/streptomycin. All cell lines were cultured to < 70% confluence for 2-3 days. All cultures were maintained at 37°C in a 5% CO_2.

Cancer and immune cells co-culture

MCF10A and T47D cells (1.5×10^6 cells/plate) were cultured in 100 mm dish overnight. Human PBMCs were purchased from Lonza (Basel, Switzerland) and cultivated in TexMACS medium supplemented with IL-7 and IL-5, followed by activation via T Cell transact with CD3 and CD28 (Miltenyi Biotec, Gaithersburg, MD, USA). Pan-T cells were expanded in TexMACS medium containing IL-7 and IL-15 prior to use. Cultured pan-T cells (1.2×10^6 cells/plate) were seeded and co-cultured for 3 days at 37°C in a 5% CO_2.

RNA isolation and quantitative RT-PCR

RNA isolation and quantitative RT-PCR were performed as previously described. Briefly, total RNA was isolated from T cells using TRIzol (Ambion, TX, USA) and the RNA was reverse transcribed into cDNA using Omniscript (QIAGEN, MD, USA) according to the manufacturer's protocol. Real-time PCR was performed in a CFX Connect (BIORAD, CA, USA) using SYBR green (Invitrogen, MA, USA) with specific primers (as listed in Supplementary Table 1). All data were normalized to RPL13A.

Cell cycle assay

Cell cycle assays were performed using propidium iodide (PI) nucleic acid staining (Invitrogen, MA, USA). T cells co-cultured with MCF10A or T47D cells were fixed with 70% ethanol for 2 h at -20°C. After fixing, wash the cells, add 50 μg/ml RNaseA, and incubate the cells for 30 min at 37°C. Then, incubate with 20 ug/ml PI for 30 min at 37°C. After staining, the cells were washed with PBS and analyzed by flow cytometry (FACS Aria II; BD Biosciences, CA, USA).

Statistics

The DESeq2 package employing the Wald statistic was used for DEGs. The FDR threshold has been described previously. One-way Analysis of variance (ANOVA) and Tukey's honest significant difference (HSD) were conducted using Prism 10.1.1. Targeted gene expression was compared between the PI and PN groups using the Student's t-test. Significance was set at * = ($P < 0.05$), ** = ($P < 0.01$) and *** = ($P < 0.001$). NS: non-significant.

Acknowledgements

This research was supported by grants from the Ministry of Science and ICT and the National Research Foundation of Korea (NRF) through the SRC program, Comparative Medicine Disease Research Center (CDRC) (2021R1A5A1033157). It was also partially supported by the Research Institute for Veterinary Science, Seoul National University.

Disclosure of conflict of interest

None.

Abbreviations

CMT, canine mammary tumor; BC, breast cancer; ICI, immune checkpoint inhibitors; PI, PBMC impaired; PN, PBMC normal-like; PBMC, peripheral blood mononuclear cells; TME, tumor microenvironment; TNBC, triple-negative breast cancer; DEG, differentially expressed gene; GO, gene ontology; TNF, tumor necrosis factor; LTB, lymphotoxin beta.

Address correspondence to: Dr. Je-Yoel Cho, Department of Biochemistry, College of Veterinary Medicine Seoul National University, Gwanak-ro1, Gwanak-gu, Seoul 08826, Republic of Korea. Tel: +82-02-880-1268; Fax: +82-02-886-1268; E-mail: jeycho@snu.ac.kr

References

[1] Siegel RL, Kratzer TB, Giaquinto AN, Sung H and Jemal A. Cancer statistics, 2025. CA Cancer J Clin 2025; 75: 10-45.
[2] Onitilo AA, Engel JM, Greenlee RT and Mukesh BN. Breast cancer subtypes based on ER/PR and Her2 expression: comparison of clinicopathologic features and survival. Clin Med Res 2009; 7: 4-13.
[3] Nure Alam Chowdhury LW, Linxia Gu and Mehmet Kaya. Exploring the potential of sensing for breast cancer detection. Appl Sci 2023; 13: 9982.
[4] Recommended breast cancer surveillance guidelines. American society of clinical oncology. J Clin Oncol 1997; 15: 2149-2156.
[5] Haber DA and Velculescu VE. Blood-based analyses of cancer: circulating tumor cells and circulating tumor DNA. Cancer Discov 2014; 4: 650-661.
[6] Burczynski ME and Dorner AJ. Transcriptional profiling of peripheral blood cells in clinical pharmacogenomic studies. Pharmacogenomics 2006; 7: 187-202.
[7] Li Y, Fan Z, Meng Y, Liu S and Zhan H. Blood-based DNA methylation signatures in cancer: a systematic review. Biochim Biophys Acta Mol Basis Dis 2023; 1869: 166583.
[8] Jin S, Sun Y, Liang X, Gu X, Ning J, Xu Y, Chen S and Pan L. Emerging new therapeutic antibody derivatives for cancer treatment. Signal Transduct Target Ther 2022; 7: 39.
[9] Pardoll DM. The blockade of immune checkpoints in cancer immunotherapy. Nat Rev Cancer 2012; 12: 252-264.
[10] Hiam-Galvez KJ, Allen BM and Spitzer MH. Systemic immunity in cancer. Nat Rev Cancer 2021; 21: 345-359.
[11] Dumeaux V, Ursini-Siegel J, Flatberg A, Fjosne HE, Frantzen JO, Holmen MM, Rodegerdts E, Schlichting E and Lund E. Peripheral blood cells inform on the presence of breast cancer: a population-based case-control study. Int J Cancer 2015; 136: 656-667.
[12] Raiter A, Lipovetzki J, Lubin I and Yerushalmi R. GRP78 expression in peripheral blood mononuclear cells is a new predictive marker for the benefit of taxanes in breast cancer neoadjuvant treatment. BMC Cancer 2020; 20: 333.
[13] Foulds GA, Vadakekolathu J, Abdel-Fatah TMA, Nagarajan D, Reeder S, Johnson C, Hood S, Moseley PM, Chan SYT, Pockley AG, Rutella S and McArdle SEB. Immune-phenotyping and transcriptomic profiling of peripheral blood mononuclear cells from patients with breast cancer: identification of a 3 gene signature which predicts relapse of triple negative breast cancer. Front Immunol 2018; 9: 2028.
[14] Nieto-Velazquez NG, Torres-Ramos YD, Munoz-Sanchez JL, Espinosa-Godoy L, Gomez-Cortes S, Moreno J and Moreno-Eutimio MA. Altered expression of natural cytotoxicity receptors and NKG2D on peripheral blood NK cell subsets in breast cancer patients. Transl Oncol 2016; 9: 384-391.
[15] Sakamoto K, Schmidt JW and Wagner KU. Mouse models of breast cancer. Methods Mol Biol 2015; 1267: 47-71.
[16] Choi Y, Lee S, Kim K, Kim SH, Chung YJ and Lee C. Studying cancer immunotherapy using patient-derived xenografts (PDXs) in humanized mice. Exp Mol Med 2018; 50: 1-9.
[17] Gray M, Meehan J, Martinez-Perez C, Kay C, Turnbull AK, Morrison LR, Pang LY and Argyle D. Naturally-occurring canine mammary tumors as a translational model for human breast cancer. Front Oncol 2020; 10: 617.
[18] LeBlanc AK and Mazcko CN. Improving human cancer therapy through the evaluation of pet dogs. Nat Rev Cancer 2020; 20: 727-742.
[19] Abadie J, Nguyen F, Loussouarn D, Pena L, Gama A, Rieder N, Belousov A, Bemelmans I, Jaillardon L, Ibisch C and Campone M. Canine invasive mammary carcinomas as models of human breast cancer. Part 2: immunophenotypes and prognostic significance. Breast Cancer Res Treat 2018; 167: 459-468.
[20] Oh JH and Cho JY. Comparative oncology: overcoming human cancer through companion animal studies. Exp Mol Med 2023; 55: 725-734.
[21] Blank CU, Haining WN, Held W, Hogan PG, Kallies A, Lugli E, Lynn RC, Philip M, Rao A, Restifo NP, Schietinger A, Schumacher TN, Schwartzberg PL, Sharpe AH, Speiser DE, Wherry EJ, Youngblood BA and Zehn D. Defining 'T cell exhaustion'. Nat Rev Immunol 2019; 19: 665-674.

[22] Newman AM, Steen CB, Liu CL, Gentles AJ, Chaudhuri AA, Scherer F, Khodadoust MS, Esfahani MS, Luca BA, Steiner D, Diehn M and Alizadeh AA. Determining cell type abundance and expression from bulk tissues with digital cytometry. Nat Biotechnol 2019; 37: 773-782.
[23] Xiao Q, Yu F, Yan L, Lao X, Liang X, Zhao H, Zhai L, Yang Z, Zhang X, Liu Y and Zhang F. The CD4/CD8 ratio is associated with T lymphocyte functions in long-term virally suppressed patients with HIV. BMC Infect Dis 2025; 25: 76.
[24] Hendriks J, Xiao Y and Borst J. CD27 promotes survival of activated T cells and complements CD28 in generation and establishment of the effector T cell pool. J Exp Med 2003; 198: 1369-1380.
[25] Harjunpaa H and Guillerey C. TIGIT as an emerging immune checkpoint. Clin Exp Immunol 2020; 200: 108-119.
[26] Leilei Z, Kewen Z, Biao H, Fang H and Yigang W. The role of chemokine IL-7 in tumor and its potential antitumor immunity. J Interferon Cytokine Res 2022; 42: 243-250.
[27] Rui R, Zhou L and He S. Cancer immunotherapies: advances and bottlenecks. Front Immunol 2023; 14: 1212476.
[28] Dempke WCM, Fenchel K, Uciechowski P and Dale SP. Second- and third-generation drugs for immuno-oncology treatment-the more the better? Eur J Cancer 2017; 74: 55-72.
[29] Lee JB, Kim HR and Ha SJ. Immune checkpoint inhibitors in 10 years: contribution of basic research and clinical application in cancer immunotherapy. Immune Netw 2022; 22: e2.
[30] Liu J, Chen Z, Li Y, Zhao W, Wu J and Zhang Z. PD-1/PD-L1 checkpoint inhibitors in tumor immunotherapy. Front Pharmacol 2021; 12: 731798.
[31] Petitprez F, Meylan M, de Reynies A, Sautes-Fridman C and Fridman WH. The tumor microenvironment in the response to immune checkpoint blockade therapies. Front Immunol 2020; 11: 784.
[32] Guo Z, Zhu Z, Lin X, Wang S, Wen Y, Wang L, Zhi L and Zhou J. Tumor microenvironment and immunotherapy for triple-negative breast cancer. Biomark Res 2024; 12: 166.
[33] MacFarlane AW 4th, Jillab M, Plimack ER, Hudes GR, Uzzo RG, Litwin S, Dulaimi E, Al-Saleem T and Campbell KS. PD-1 expression on peripheral blood cells increases with stage in renal cell carcinoma patients and is rapidly reduced after surgical tumor resection. Cancer Immunol Res 2014; 2: 320-331.
[34] Liu JN, Kong XS, Huang T, Wang R, Li W and Chen QF. Clinical implications of aberrant PD-1 and CTLA4 expression for cancer immunity and prognosis: a pan-cancer study. Front Immunol 2020; 11: 2048.
[35] Jiang Y, Li Y and Zhu B. T-cell exhaustion in the tumor microenvironment. Cell Death Dis 2015; 6: e1792.
[36] Chow L, Wheat W, Ramirez D, Impastato R and Dow S. Direct comparison of canine and human immune responses using transcriptomic and functional analyses. Sci Rep 2024; 14: 2207.
[37] Kim ES, Kim SY and Moon A. C-reactive protein signaling pathways in tumor progression. Biomol Ther (Seoul) 2023; 31: 473-483.
[38] Shin JW, Kim N, Minh NT, Chapagain DD and Jee SH. Serum bilirubin subgroups and cancer risk: insights with a focus on lung cancer. Cancer Epidemiol 2025; 94: 102727.
[39] Dai E, Zhu Z, Wahed S, Qu Z, Storkus WJ and Guo ZS. Epigenetic modulation of antitumor immunity for improved cancer immunotherapy. Mol Cancer 2021; 20: 171.
[40] Ababneh O, Nishizaki D, Kato S and Kurzrock R. Tumor necrosis factor superfamily signaling: life and death in cancer. Cancer Metastasis Rev 2024; 43: 1137-1163.
[41] Wang Z, Zhu J, Wang T, Zhou H, Wang J, Huang Z, Zhang H and Shi J. Loss of IL-34 expression indicates poor prognosis in patients with lung adenocarcinoma. Front Oncol 2021; 11: 639724.
[42] Wen Z, Liu T, Xu X, Acharya N, Shen Z, Lu Y, Xu J, Guo K, Shen S, Zhao Y, Wang P, Li S, Chen W, Li H, Ding Y, Shang M, Guo H, Hou Y, Cui B, Shen M, Huang Y, Pan T, Qingqing W, Cao Q, Wang K and Xiao P. Interleukin-16 enhances anti-tumor immune responses by establishing a Th1 cell-macrophage crosstalk through reprogramming glutamine metabolism in mice. Nat Commun 2025; 16: 2362.
[43] Murilo Porfírio de Aguiar JHV. Entrance to the multifaceted world of CD4+ T cell subsets. Explor Immunol 2024; 4: 152-168.
[44] Lee KH, Park HM, Son KH, Shin TJ and Cho JY. Transcriptome signatures of canine mammary gland tumors and its comparison to human breast cancers. Cancers (Basel) 2018; 10: 317.
[45] Ge SX, Son EW and Yao R. iDEP: an integrated web application for differential expression and pathway analysis of RNA-Seq data. BMC Bioinformatics 2018; 19: 534.
[46] Chen EY, Tan CM, Kou Y, Duan Q, Wang Z, Meirelles GV, Clark NR and Ma'ayan A. Enrichr: interactive and collaborative HTML5 gene list enrichment analysis tool. BMC Bioinformatics 2013; 14: 128.
[47] Chen B, Khodadoust MS, Liu CL, Newman AM and Alizadeh AA. Profiling tumor infiltrating immune cells with CIBERSORT. Methods Mol Biol 2018; 1711: 243-259.

A

	CCRCDID	Group	Breed	Sex	Spay	Age
1	CCRCD0008	M	Schnauzer	F	O	15
2	CCRCD0009	M	Maltese	F		11
3	CCRCD0010	M	Cocker spaniel	F	O	10
4	CCRCD0012	M	Dachshund	F		11
5	CCRCD0021	M	Pomeranian	F	O	13
6	CCRCD0047	M	Schnauzer	F	O	13
7	CCRCD0052	M	Maltese	F		12
8	CCRCD0053	M	Jindo	F	O	13
9	CCRCD0070	M	Maltese	F	O	12
10	CCRCD0088	M	Schnauzer	F	O	9
11	CCRCD0094	M	Shih-tzu	F	O	11
12	CCRCD0095	M	Maltese	F	O	11
13	CCRCD0105	M	Jindo	F	O	13
14	CCRCD0107	M	Cocker spaniel	F	O	14
15	CCRCD0117	M	Maltese	F	O	10
16	CCRCD0128	M	Shih-tzu	F	O	14
17	CCRCD0132	M	Maltese	F		11
18	CCRCD0138	M	Mixed	F	O	9
19	CCRCD0143	M	Shih-tzu	F		15
20	CCRCD0148	M	Chihuahua	F		10
21	CCRCD0149	M	Cocker spaniel	F		11
22	CCRCD0151	M	Dachshund	F		15
23	CCRCD0153	M	Maltese	F	O	7
24	CCRCD0157	M	Samoyed	F		13
25	CCRCD0162	M	Maltese	F	O	11
26	CCRCD0165	M	Poodle	F		5
27	CCRCD0166	M	Dachshund	F		7
28	CCRCD0167	M	Poodle	F		12
29	CCRCD0184	M	Yorkshire Terrier	F		14
30	CCRCD0018	B	Mixed	F	O	10
31	CCRCD0024	B	Maltese	F		11
32	CCRCD0029	B	Maltese	F		10
33	CCRCD0034	B	Shih-tzu	F	O	10
34	CCRCD0050	B	Poodle	F		14
35	CCRCD0072	B	Maltese	F	O	11
36	CCRCD0073	B	Maltese	F		8
37	CCRCD0087	B	Maltese	F		10
38	CCRCD0091	B	Maltese	F		16
39	CCRCD0096	B	Yorkshire Terrier	F		5
40	CCRCD0099	B	Cocker spaniel	F	O	14
41	CCRCD0101	B	Maltese	F	O	10
42	CCRCD0104	B	Maltese	F	O	10
43	CCRCD0109	B	Maltese	F		9
44	CCRCD0110	B	Bichon Frise	F	O	10
45	CCRCD0120	B	Pomeranian	F		8
46	CCRCD0137	B	Maltese	F		10
47	CCRCD0145	B	Old english sheep dog	F	O	7
48	CCRCD0158	B	Yorkshire Terrier	F	O	8
49	CCRCD0159	B	Maltese	F		7
50	CCRCD0161	B	Dachshund	F		8
51	CCRCD0179	B	Schnauzer	F	O	17
52	CCRCD0185	B	Maltese	F	O	14
53	CCRCD0192	B	Poodle	F	O	9
54	CCRCD0193	B	Maltese	F	O	11
55	CCRCD0324	N	Mixed	F	O	9
56	CCRCD0332	N	Maltese	F	O	9
57	CCRCD0360	N	Dachshund	F	O	8
58	CCRCD0370	N	Cocker spaniel	F	O	9
59	CCRCD0413	N	Mixed	F	O	4
60	CCRCD0414	N	Mixed	F	O	4
61	CCRCD0518	N	Chihuahua	F	O	12
62	CCRCD0555	N	Poodle	F	O	11

B

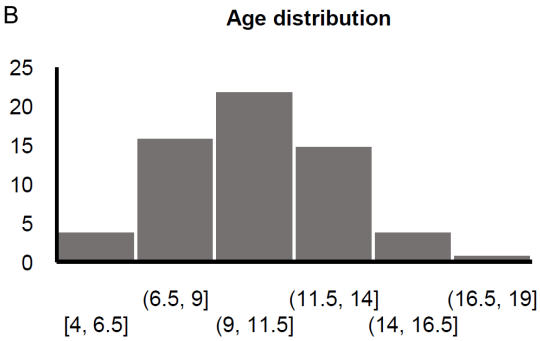

C

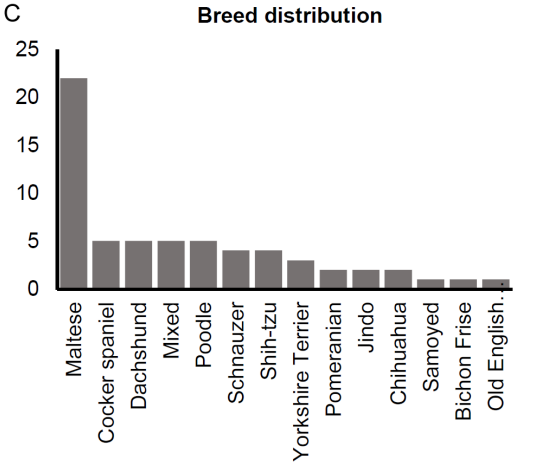

D

Group	
Malignant	29
Benign	25
Normal	8

Subtypes	
Complex type	21
Ductal type	2
Lobular hyperplasia	1
Mixed type	7
Simple type	4
Special type	3
Unknown	16
Healthy	8

Supplementary Figure 1. Companion dogs enrolled in the dog CMT project. A. 62 companion dogs that participated in this study were listed according to tumor type (M and B) or normal (N), breed, sex, spay, and age. B. Age distribution of the enrolled dogs. 9 to 11.5 years old were the most prevalent. C. Maltese had the highest number of dog breeds. D. Summary of cancer subtypes shows that complex types followed by mixed types of tumors are frequently found in specimens.

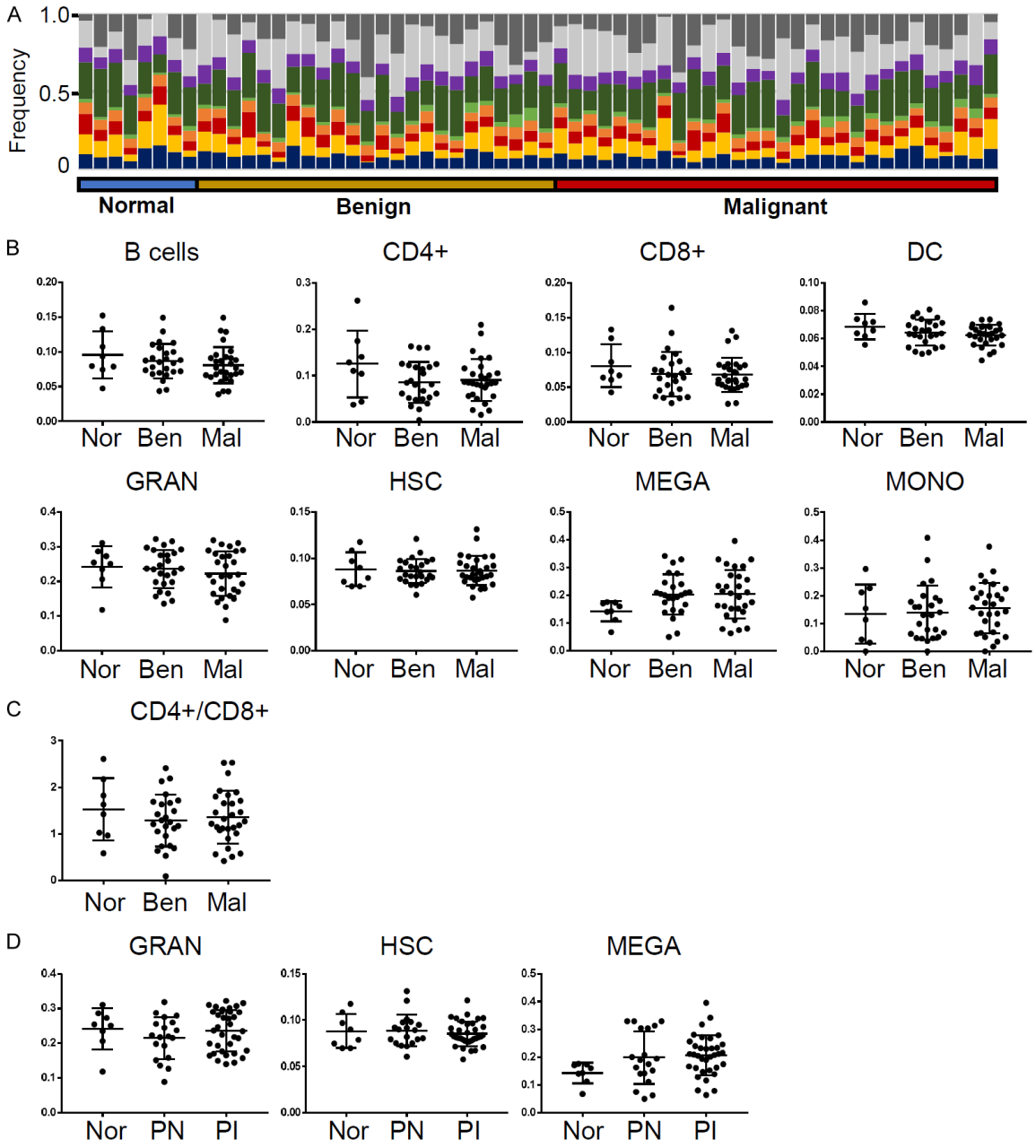

Supplementary Figure 2. Deconvolution defined cell type distribution in normal, benign and malignant classification. A. Cell population in a 100 percent stacked bar chart assessed by deconvolution of bulk PBMC transcriptome data in normal, benign, and malignant groups of dogs. B. Scatter dot plot with mean values and standard deviation (SD) in the normal (Nor), benign (Ben), and malignant (Mal) groups. DC, dendritic cells; GRAN, granulocytes; HSC, human stem cells; MEGA, megakaryocytes; MONO, monocytes. C. CD4+/CD8+ cell ratios in the normal, benign, and malignant groups. D. GRAN, HSC, and MEGA cells in the normal (Nor), PN (PBMC-normal like), and PI (PBMC-impaired) groups. No significant differences were found among the groups.

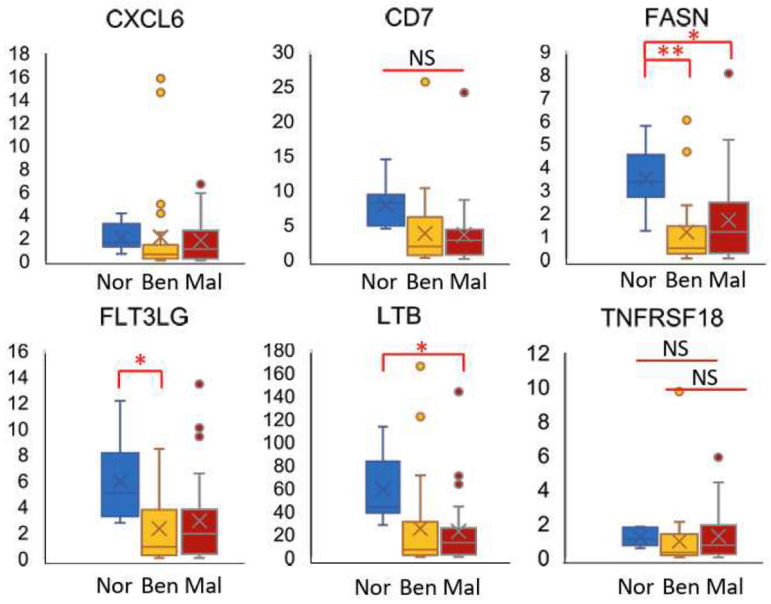

Supplementary Figure 3. Expression profiles of six signature genes in tumor-based classification. The expression patterns of six signature genes identified from PBMC transcriptome-based classification in tumor-based classification. Significance was tested and set at *= ($P < 0.05$), **= ($P < 0.01$) and ***= ($P < 0.001$). NS: nonsignificant.

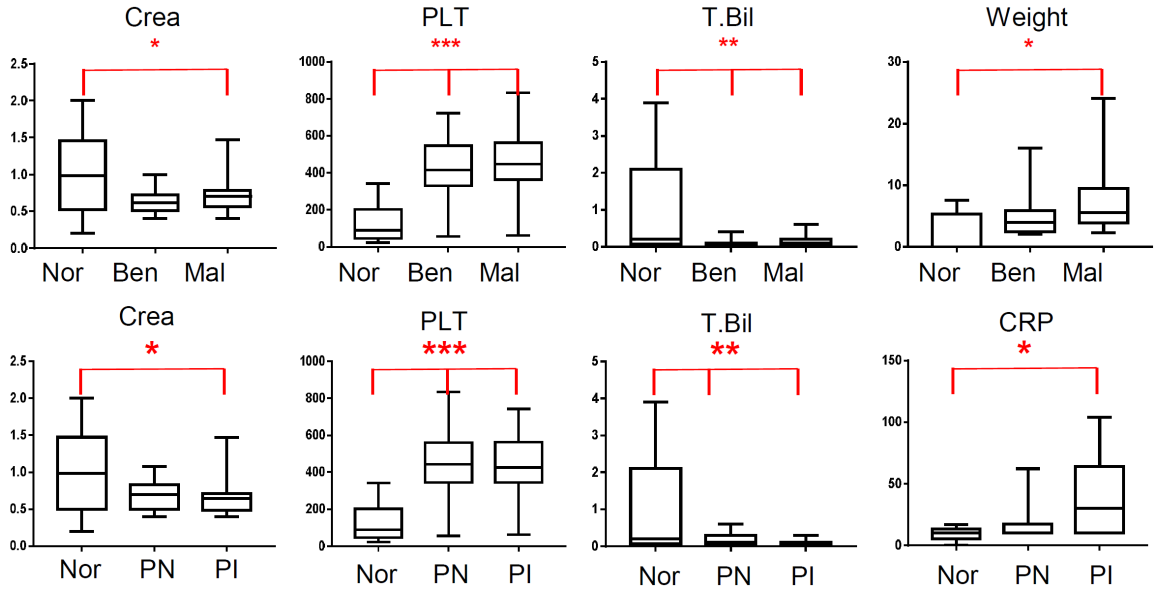

Supplementary Figure 4. Significant difference in clinical characteristics of routine blood test results among three groups. Crea (creatinine) and total bilirubin (T. Bil) levels were lower in both cancer type-based classification (benign and malignant) and unsupervised clustering (PN and PI) groups than in the normal group. In contrast, PLT (platelet) count was higher in the normal group than in the other groups. However, C-reactive protein (CRP) was significantly higher in the PI group than in the normal group.

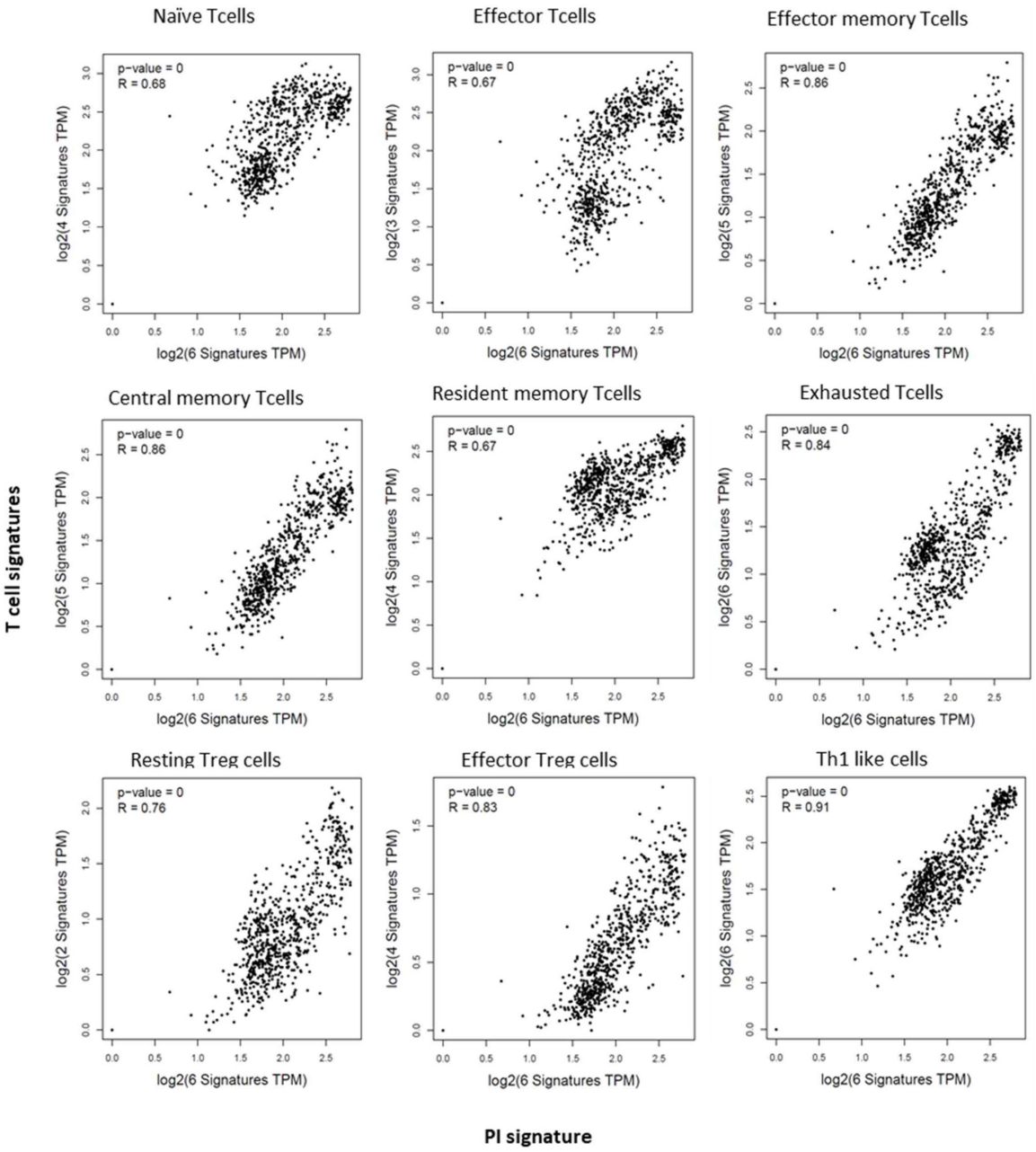

Supplementary Figure 5. The correlation between the PI signature and T cell signatures was analyzed by comparing the gene expression of nine different T cell signatures with the expression of CD7, CXCL6, FASN, FLT3LG, LTB, and TNFRSF18 in the whole blood GTX database.

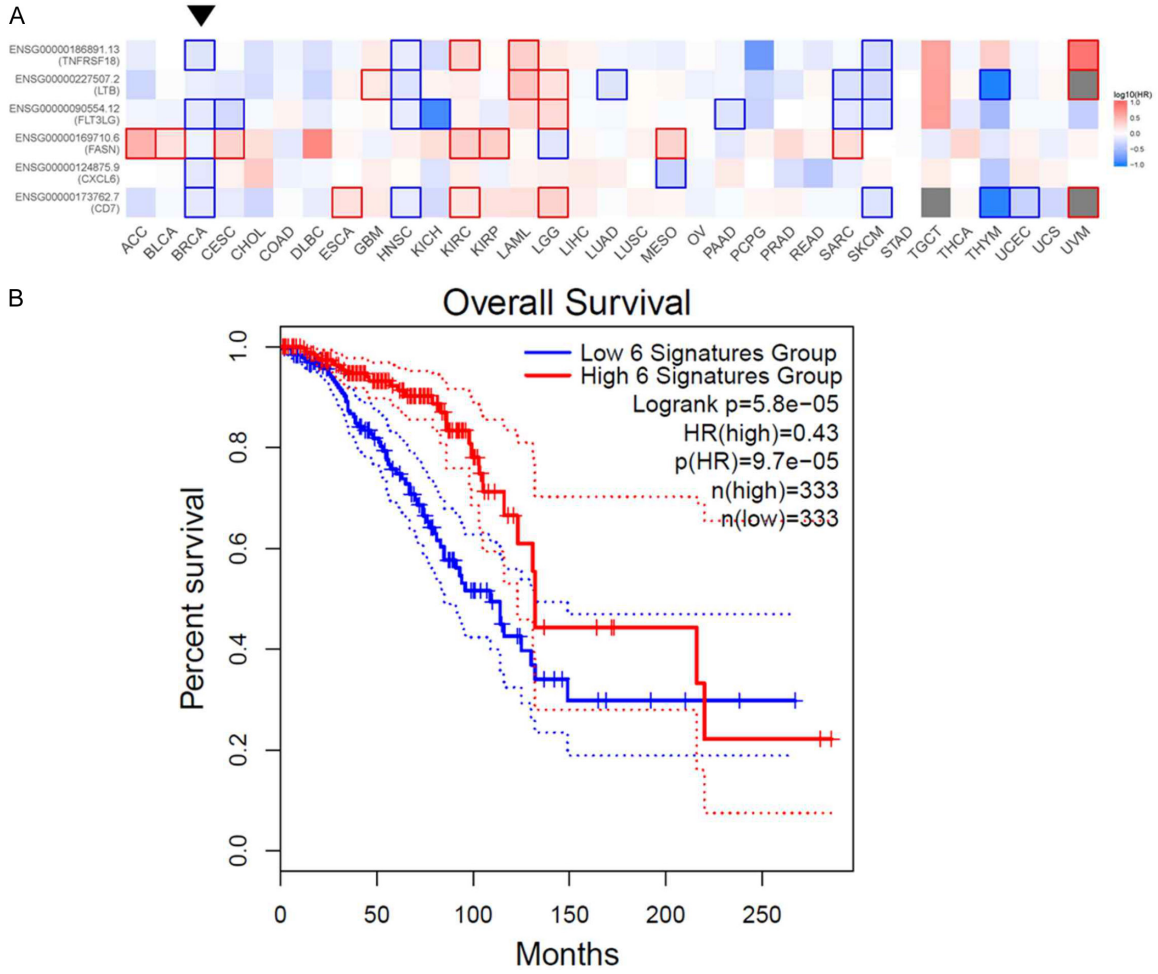

Supplementary Figure 6. Association between PI signature gene expression and survival in cancer patients. A. A heatmap illustrates the positive (red) and negative (blue) associations between PI signature gene expression and patient survival across 33 different cancer databases. Statistically significant associations are high lighted with square frames. Notably, PI signature gene expression shows a strong negative correlation with survival in breast cancer patients. B. The overall survival rate of breast cancer patients stratified by high PI signature gene expression is shown using a Kaplan-Meier plot.

Supplementary Table 1. List of primers

Gene	Direction	Sequence	Size	Tm
Cxcl6	F	TTGGTAAACTGCAGGTGTTCCC	89	60
	R	CAGACAAACTTGCTTCCCGTTC		59.3
Cd7	F	GGGGTCCTGTAGACCCAGAG	70	59.7
	R	CCATGTTCCCCACACCCAG		59.3
Fasn	F	AACTCCTTGGCGGAAGAGA	150	57.3
	R	TAGGACCCCGTGGAATGTCA		59.3
Ltb	F	GAGGACTGGTAACGGAGACG	100	58.6
	R	GGGCTGAGATCTGTTTCTGG		57
Flt3lg	F	CTGGATCACTCGCCAGAACT	70	58.5
	R	TGGCAGGGTTGAGGAGTC		57.5
Tnfrsf18 (Cd357)	F	TGAATTCCACTGCGGAGACC	172	59.1
	R	GCAGTCTGTCCAAGGTTTGC		58.7
Tight	F	CGTGAACGATACAGGGGAGT	131	58.2
	R	GCAATGGAATCTGGAACCTG		55.8
Cd27	F	AACTCTGGTCTTCTCGTTCGCA	112	60.9
	R	TTGGAAGAGGATCACACTCGGT		60.1
Il7	F	TTGCCAAGGCGTTGAGAGAT	120	59
	R	CCTGGATGAGGACCAGAGGA		59
Actb	F	ACAGAGCCTCGCCTTTG	110	55.8
	R	CCTTGCACATGCCGGAG		57.5

Primers targeting 20 genes are listed with direction, sequence, expected amplicon size, and Tm.